



HF
15,7

654

Received November 2003
Revised November 2004
Accepted November 2004

Steady mixed convection flow of a micropolar fluid near the stagnation point on a vertical surface

Y.Y. Lok

*Academic Service Center, Kolej Universiti Teknikal Kebangsaan Malaysia,
Melaka, Malaysia*

N. Amin

Department of Mathematics, Universiti Teknologi Malaysia, Johor, Malaysia, and

D. Campean and I. Pop

Faculty of Mathematics, University of Cluj, Cluj, Romania

Abstract

Purpose – To study the steady mixed convection boundary-layer flow of a micropolar fluid near the region of the stagnation point on a double-infinite vertical flat plate is studied. The results of this paper are important for the researchers in the area of micropolar fluids.

Design/methodology/approach – For the case considered the problem reduces to a system of ordinary differential equations, which is solved numerically using the Keller-box method. This method is very efficient for solving boundary-layer problems and it can easily be applied to other general situations than that presented in this paper. Any PhD student can learn and apply it very easily.

Findings – Representative results for the velocity, microrotation and temperature profiles, as well as for the reduced skin friction coefficient and the local Nusselt number have been obtained for the case of strong concentration, Prandtl number of 0.7, some values of the material parameter K and the mixed convection parameter $\lambda (\geq 0)$. Both assisting and opposing flow cases are considered. Results for the reduced skin friction coefficient and reduced local Nusselt number as well as for the reduced velocity, temperature and microrotation profiles are given in tables and figures. The obtained results are compared with ones from the open literature and it is found that they are in excellent agreement. The important conclusion is, we have been able to show that for opposing flow solutions are possible are possible only for a limited range of values of the mixed convection parameter λ .

Research limitations/implications – The results of this paper are valid only in the small region around the stagnation point on a vertical surface and they are not applicable outside this region.

Practical implications – The theory of micropolar fluids and also the results of the present paper can be used to explain the characteristics in certain fluids such as exotic lubricants, colloidal suspensions or polymeric fluids, liquid crystals, and animal blood.

Originality/value – The paper is very well prepared, presented and readable. We believe that the results are original and important from both theoretical and application point of views.

Keywords Convection, Boundary layers, Fluids, Flow

Paper type Research paper



Nomenclature

C_f	= skin friction coefficients	U_e	= reference velocity
f	= reduced stream function	x, y	= Cartesian coordinates along the wall and normal to it, respectively
g	= gravitational acceleration		
Gr	= Grashof number		
h	= reduced microrotation		
j	= microinertia density	<i>Greek symbols</i>	
K	= material parameter	γ	= spin gradient viscosity
L	= reference length	β	= thermal expansion coefficient
n	= ratio of the microrotation vector component and the fluid skin friction at the wall	η	= transformed variable
N	= component of the microrotation vector normal to x - y plane	θ	= dimensionless temperature
Nu	= Nusselt number	λ	= mixed convection parameter
Pr	= Prandtl number	κ	= vortex viscosity
Re	= Reynolds number	μ	= viscosity
T	= fluid temperature	ν	= kinematic viscosity
T_0	= reference temperature	ρ	= density
$T_w(x)$	= surface temperature		
u, v	= velocity components along x and y axes	<i>Subscripts</i>	
$u_e(x)$	= free stream velocity	e	= boundary-layer edge condition
		w	= wall condition
		∞	= far field condition
		<i>Superscript</i>	
		'	= differentiation with respect to η

Introduction

During recent years the theory of micropolar fluids has received much attention and this is because the traditional Newtonian fluids cannot precisely describe the characteristics of the fluid flow with suspended particles. Physically micropolar fluids may be described as the non-Newtonian fluids consisting of dumb-bell molecules or short rigid cylindrical elements, polymer fluids, fluid suspensions, animal blood, etc. The presence of dust or smoke, particularly in a gas, may also be modeled using micropolar fluid dynamics. The theory of micropolar fluids, first proposed by Eringen (1966, 1972), is capable of describing such fluids. In this theory the local effects arising from the microstructure and the intrinsic motion of the fluid elements are taken into account. This is a kind of continuum mechanics, and many classical flows are being re-examined to determine the effects of fluid microstructure (Willson, 1970; Bergholz, 1980; Chandra Shekar *et al.*, 1984). Early studies along these lines may be found in the review article by Peddieson and McNitt (1970), and in the recent books by lukaszewicz (1999) and Eringen (2001). Gorla (1983), Kumari and Nath (1984) and Guram and Smith (1980) were the first to apply the micropolar boundary-layer theory to problems of steady and unsteady stagnation point flows and they claimed that the micropolar fluid model is capable of predicting results which exhibit turbulent flow characteristics, although it is difficult to see how a steady laminar boundary-layer flow could appear to be turbulent. Studies of micropolar fluids have recently received considerable attention due to their application in a number of processes that occur in industry. Such applications include the extrusion of polymer fluids, solidification of liquid crystals, cooling of a metallic plate in a bath, animal bloods, exotic lubricants and colloidal and suspension solutions, for example, for which the classical Navier-Stokes theory is inadequate.

The aim of the present paper is to study the steady mixed convection boundary-layer flow of a micropolar fluid near the stagnation point on a double-infinite vertical surface with a free stream velocity $u_e(x)$ and a prescribed surface temperature $T_w(x)$. However, only the case when $T_w(x)$ varies linearly with the distance along the plate, x , is considered. It is shown that for this case the partial differential equations governing the fluid flow and heat transfer reduce to a set of ordinary differential equations, which have been solved numerically using an implicit finite-difference scheme known as the Keller-box scheme. Mixed convection in stagnation flows is important when the buoyancy forces, due to the temperature difference between the wall and the free stream, become high and thereby modify the flow and thermal fields significantly. In addition, the local heat transfer rate and local shear stress can be significantly enhanced or diminished in comparison to the pure forced convection case. It should, however, be mentioned that in such flows, the flow and thermal fields are no longer symmetric with respect to the stagnation line.

Governing equations

Consider a double-infinite vertical flat plate, which is placed in a micropolar fluid of uniform ambient temperature T_∞ . It is assumed that the temperature of the plate is $T_w(x)$ and the velocity of the external flow is $u_e(x)$. However, only the case when the temperature of the plate varies linearly with the distance x is considered. The flow configuration is shown schematically in Figure 1 together with the corresponding Cartesian coordinates in the vertical and horizontal directions.

Thus, the plate temperature and the condition far from the plate is assumed to be given by

$$T_w(x) = T_\infty + T_0(x/L), \quad u_e(x) = U_e(x/L) \tag{1}$$

where U_e is a reference velocity, L is a characteristic length and $T_0 > 0$ is a reference temperature. Under the boundary layer and Boussinesq assumptions, the

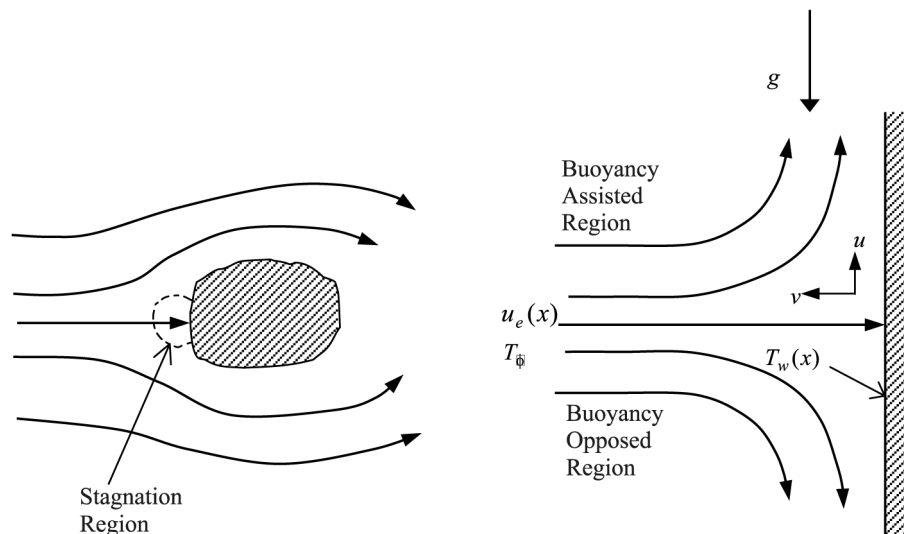


Figure 1.
Physical model and
coordinate system

steady laminar boundary-layer equations governing the mixed convection flow are given by

Convection flow
of a micropolar
fluid

$$\frac{\partial u}{\partial x} + \frac{\partial v}{\partial y} = 0 \quad (2)$$

$$u \frac{\partial u}{\partial x} + v \frac{\partial u}{\partial y} = u_e \frac{du_e}{dx} + \left(\frac{\mu + \kappa}{\rho} \right) \frac{\partial^2 u}{\partial y^2} + \frac{\kappa}{\rho} \frac{\partial N}{\partial y} \pm g\beta(T - T_\infty) \quad (3)$$

$$\rho j \left(u \frac{\partial N}{\partial x} + v \frac{\partial N}{\partial y} \right) = -\kappa \left(2N + \frac{\partial u}{\partial y} \right) + \gamma \frac{\partial^2 N}{\partial y^2} \quad (4)$$

$$u \frac{\partial T}{\partial x} + v \frac{\partial T}{\partial y} = \frac{\nu}{Pr} \frac{\partial^2 T}{\partial y^2} \quad (5)$$

657

subject to the boundary conditions:

$$\begin{aligned} u(x, 0) &= v(x, 0) = 0, \\ N(x, 0) &= -n \frac{\partial u}{\partial y}(x, 0), \quad x \geq 0 \\ T(x, 0) &= T_w(x) = T_\infty + T_o(x/L), \quad x \geq 0 \\ u(x, \infty) &= u_e(x) = U_e(x/L), \\ N(x, \infty) &= 0, \\ T(x, \infty) &= T_\infty, \quad x \geq 0 \end{aligned} \quad (6)$$

where u and v are the velocity components along the x and y axes, respectively, N is the component of the microrotation vector normal to the x - y plane, T is the fluid temperature, g is the magnitude of the acceleration due to gravity, ρ is the density, μ is the absolute viscosity, κ is the vortex viscosity, γ is the spin-gradient viscosity, ν is the kinematic viscosity, j is the microinertia density, Pr is the Prandtl number and n is a constant such that $0 \leq n \leq 1$. It should be mentioned that the case $n = 0$, called strong concentration by Guram and Smith (1980), indicates $N = 0$ near the wall, represents concentrated particle flows in which the microelements close to the wall surface are unable to rotate (Jena and Mathur, 1981). The case $n = 1/2$ indicates the vanishing of anti-symmetrical part of the stress tensor and denotes weak concentration (Ahmadi, 1976). The case $n = 1$, as suggested by Peddieson (1972), is used for the modelling of turbulent boundary-layer flows. We shall consider here only the values of $n = 0$ (strong concentration). Also, the plus and minus signs in equation (3) pertain, respectively, to the buoyancy assisting and the buoyancy opposing flow regions. Figure 1 shows such a flow field for a vertical, heated surface with the upper half of the flow field being assisted and the lower half of the flow field being opposed by the buoyancy force. The reverse trend will occur if the plate is cooled below the ambient temperature T_∞ . Our results will thus be true for both the heated and cooled surface conditions when the appropriate (assisting and opposing) flow regions are selected.

We introduce now the following similarity variables

$$\begin{aligned} \eta &= (U_e/L\nu)^{1/2}y, \quad u(x,y) = U_e(x/L)f'(\eta), \quad v(x,y) = -(U_e\nu/L)^{1/2}f(\eta) \\ N(x,y) &= (U_e/L)(U_e/L\nu)^{1/2}(x/L)h(\eta), \quad T(x,y) = T_\infty + T_0(x/L)\theta(\eta) \quad (7) \\ \lambda &= Gr/Re^2, \quad Gr = g\beta T_0 L^3/\nu^2, \quad Re = U_e L/\nu \end{aligned}$$

where Gr is the Grashof number, Re is the Reynolds number, λ (= constant) and positive is the mixed convection parameter and prime denotes differentiation with respect to η .

We follow the work of many recent authors by assuming that γ is given by, see Rees and Bassom (1996) or Rees and Pop (1998),

$$\gamma = (\mu + \kappa/2)j = \mu(1 + K/2)j \quad (8)$$

where $K = \kappa/\mu$ is the material parameter. Using equations (7) and (8) in equations (2)-(5), we get

$$(1 + K)f''' + ff'' + 1 - f'^2 + Kh' \pm \lambda\theta = 0 \quad (9)$$

$$\left(1 + \frac{K}{2}\right)h'' + fh' - f'h - K(2h + f'') = 0 \quad (10)$$

$$\frac{1}{Pr}\theta'' + f\theta' - f'\theta = 0 \quad (11)$$

subject to the boundary conditions:

$$\begin{aligned} f(0) = f'(0) = 0, \quad \theta(0) = 1, \quad h(0) = -nf''(0) \\ f' \rightarrow 1, \quad \theta \rightarrow 0, \quad h \rightarrow 0 \quad \text{as } \eta \rightarrow \infty \end{aligned} \quad (12)$$

It should be noted that for $K = 0$ (Newtonian fluid), equations (9-11) reduce to those found by Ramachandran *et al.* (1988) for the power law temperature $T_w(x) = T_\infty + bx^n$ with $n = 1$ in their equations (17) and (18).

Of interest in this problem is also the skin friction coefficient, which can be expressed as

$$C_f = \frac{(x/L)}{\frac{1}{2}\rho U_e^2(x)} \left\{ (\mu + \kappa) \frac{\partial u}{\partial y} + \kappa N \right\}_{y=0} = 2Re^{-1/2} \{1 + (1 - n)K\} f''(0)$$

Similarly, the heat transfer coefficient in terms of the Nusselt number can be written as

$$Nu = \frac{L}{T_w - T_\infty} \left(-\frac{\partial T}{\partial y} \right)_{y=0} = Re^{1/2} [-\theta'(0)] \quad (14)$$

Results and discussion

Equations (9-11), subject to the boundary conditions (12), were solved numerically using a very efficient implicit finite-difference method, namely the Keller-box method, in conjunction with the Newton's linearization technique as described by Cebeci and

Bradshaw (1984). Representative results for the velocity, microrotation and temperature profiles, as well as for the reduced skin friction coefficient and the local Nusselt number have been obtained for $n = 0$ (strong concentration), $Pr = 0.7$ and some values of the material parameter K and the mixed convection parameter $\lambda(\geq 0)$. However, it should be mentioned that all of the results that are presented here are valid only in the small region around the stagnation point and they are not applicable outside this region.

Results for the reduced skin friction coefficient, $f''(0)$, and the reduced local Nusselt number, $-\theta'(0)$, are given in Table I for $n = 0$, $K = 0$ (Newtonian fluid) and $\lambda = 1$ when the Prandtl number varies in the range $0.7 \leq Pr \leq 100$. Both the cases of assisting and opposing flows are considered. The values found by Ramachandran *et al.* (1988) have also been included in this table and it is seen that there is an excellent agreement between these results. Also, it is noticed, as expected, that when the value of Pr increases, the thermal boundary-layer thickness decreases and this leads to an increase in the local Nusselt number. The trends are reverse for buoyancy assisting and buoyancy opposing flow cases. For opposing flow, the reduced skin friction coefficient increases as the Prandtl number increases. However, the same trends happen for the local Nusselt number in the both buoyancy assisting and opposing flow cases. These behaviours are observed for both buoyancy assisting and opposing flow cases with the latter case having lower values of the reduced skin friction coefficient and the local Nusselt number than the former case.

The variation of the reduced skin friction coefficient, $f''(0)$, and the reduced local Nusselt number, $-\theta'(0)$, with the mixed convection parameter $\lambda(\geq 0)$ are shown in Figures 2 and 3, respectively, for $n = 0$ (strong concentration), $Pr = 0.7$ and some values of the material parameter K . Values of $f''(0)$ and $-\theta'(0)$ are also given in Table II but only for the opposing flow situation. These figures show that in the case of assisting flow, values of $f''(0)$ and $-\theta'(0)$ increase, this increase being substantial in comparison to the case of forced convection flow ($\lambda = 0$). This may be attributed to the increase in the velocity caused by the assisting buoyancy forces. However, values of $f''(0)$ and $-\theta'(0)$ decrease as the material parameter K increases. On the other hand, for the buoyancy opposing flow situation, the adverse pressure gradient increases as the mixed convection parameter λ increases, and this causes the flow to separate and eventually to reverse, i.e. the local skin friction, $f''(0)$, and the local Nusselt number, $-\theta'(0)$, become zero for some values of λ , see Figures 2 and 3. The values of λ for which $f''(0) = 0$ and $-\theta'(0) = 0$ are given in Table III. Thus the assisting flow leads to a direct heat flow ($-\theta'(0) > 0$), i.e. from the wall to the surrounding fluid, while the

Pr	Buoyancy assisting flow		Buoyancy opposing flow	
	$f''(0)$	$-\theta'(0)$	$f''(0)$	$-\theta'(0)$
0.7	1.706376 (1.7063)	0.764087 (0.7641)	0.691693 (0.6917)	0.633269 (0.6332)
7	1.517952 (1.5179)	1.722775 (1.7224)	0.923528 (0.9235)	1.546374 (1.5403)
20	1.448520 (1.4485)	2.458836 (2.4576)	1.003158 (1.0031)	2.269380 (2.2683)
40	1.410094 (1.4101)	3.103703 (3.1011)	1.045989 (1.0459)	2.907781 (2.9054)
60	1.390311 (1.3903)	3.555404 (3.5514)	1.067703 (1.0677)	3.356338 (3.3527)
80	1.377429 (1.3774)	3.914882 (3.9095)	1.081719 (1.0817)	3.713824 (3.7089)
100	1.368070 (1.3680)	4.218462 (4.2116)	1.091840 (1.0918)	4.015974 (4.0097)

Note: () Results by Ramachandran *et al.* (1988)

Table I.
Values of $f''(0)$ and $-\theta'(0)$
for $K = 0$ (Newtonian
fluid), $\lambda = 1$, $n = 0$ and
some values of Pr when
the flow is buoyancy
assisting or buoyancy
opposing, respectively

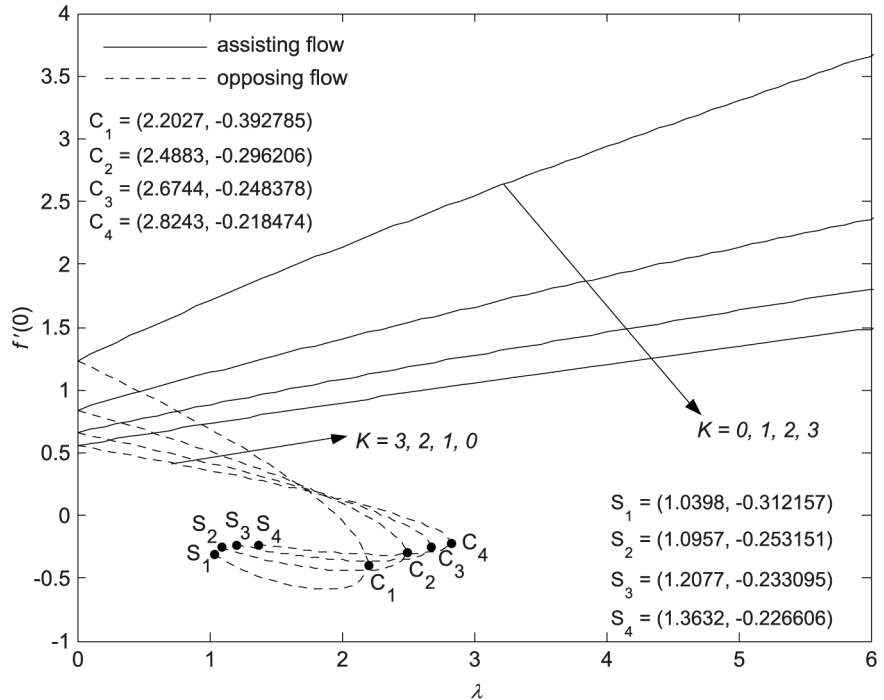


Figure 2.
Variation of $f''(0)$ with λ for $Pr = 0.7$ and some values of K

opposing flow leads to a reversed heat flow ($-\theta'(0) < 0$), i.e. from the surrounding fluid to the wall, respectively. We also notice that solutions do not exist beyond some critical value of the parameter λ . Turning (or critical) points C_i ($i = 1, 2, 3, 4$) occur before the singular points S_i ($i = 1, 2, 3, 4$) are reached, and dual solutions exist for some values of λ when the flow is opposed. It should be mentioned that it is very difficult to obtain the exact coordinates for the points S_i . The computations have been performed until a singularity occurs at these points, i.e. where the solution does not converge, and the calculations were terminated at this location. Further, it is seen that in the case of opposing flow the values of the ordinates of all singular points S_i ($i = 1, 2, 3, 4$) are negative for both the reduced skin friction coefficient, $f''(0)$, and reduced local Nusselt number, $-\theta'(0)$ for the values of n and of the material parameter K considered. However, the values of the coordinates of the critical points C_i ($i = 1, 2, 3, 4$) are negative for the reduced skin friction coefficient, $f''(0)$, while they are positive for the reduced local Nusselt number, $-\theta'(0)$, for the values of n and K considered. To this end, we also notice from Figures 2 and 3 that for some values of λ when the flow is opposing, the reduced skin friction, $f''(0)$, and local Nusselt number, $-\theta'(0)$, decrease and for other values of λ they increase with increase in the material parameter K .

Representative velocity, temperature and microrotation profiles are shown in Figures 4-14 for $n = 0$ (strong concentration), $Pr = 0.7$ and some values of the parameters K and λ . The first and second (dual) solutions are also shown in these figures for the case of opposing flow with $\lambda = 1.5, 2, 2.2, 2.4$ and 2.5 . It is seen from Figures 4, 5, 6, 8 and 9 that as the material parameter K increases, the velocity profiles

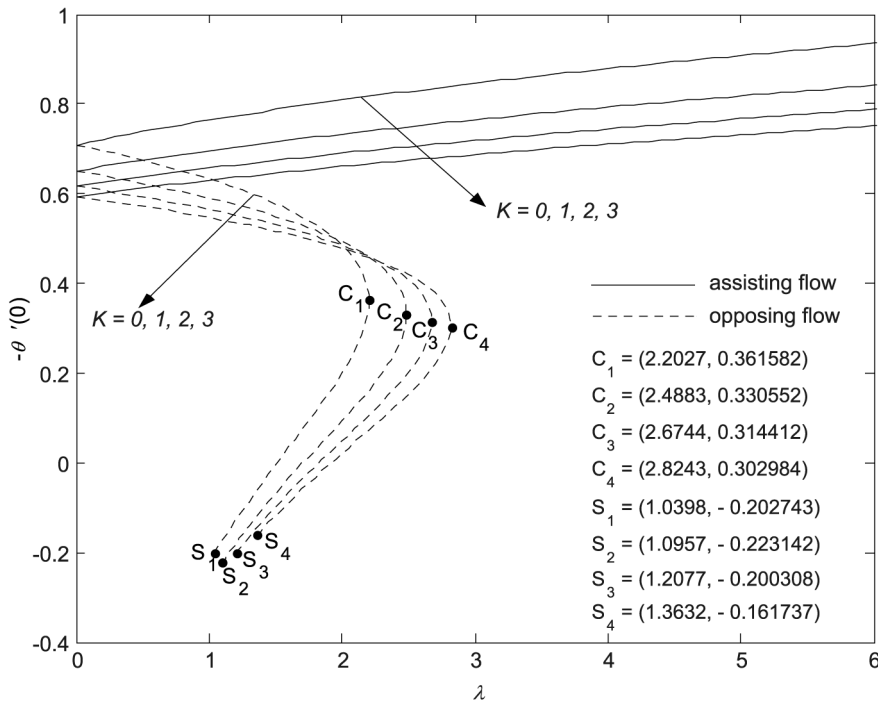


Figure 3.
Variation of $-\theta'(0)$ with λ
for $Pr = 0.7$ and some
values of K

$f(\eta)$ are found to diminish and the peak velocity decreases, while the temperature profiles $\theta(\eta)$ increase. Therefore, the parameter K has a retarding effect on the flow field. However, the peak values of the microrotation profiles $h(\eta)$ shown in Figures 7 and 10 increase as K increases. It is also observed from Figures 4, 5, 6, 8, 9 and 11 that the velocity and temperature profiles for the micropolar fluid ($K > 0$) are larger than that for the Newtonian fluid ($K = 0$). This phenomenon reflects the fact that increasing the value of K results in an enhancement of the total viscosity in the fluid flow, thus decreasing the velocity and the heat transfer rate. The decrease of the velocity profiles owing to the influence of vortex viscosity gives rise to the less heat transfer rate from the wall, thus increasing the hydrodynamic and thermal boundary-layer thicknesses. Further, we observe from Figures 7, 10 and 13 that the microrotation gradient h' is negative near the plate and it gradually increases, i.e. accelerates the fluid far away from the plate. The term Kh' in equation (9) shows that a negative microrotation gradient retards the fluid far away from the plate, while a positive microrotation gradient accelerates the fluid far away from the plate. This is not surprising since for a given Prandtl number Pr , the fluid effectively becomes more "viscous" with increasing K values (note the coefficient of the diffusing term in equation (9)). Consequently, the velocity gradient at the wall decreases, with an accompanying increase in the momentum boundary-layer thickness. This behaviour is also observed in the case of temperature profiles shown in Figures 5, 8 and 11. All these observations are in agreement with the results reported by Cheng and Wang (2000) for the forced convection in micropolar fluid flow over a wavy surface. Finally,

Table II.
Values of $f''(0)$ and $-\theta'(0)$ for different values of λ with $Pr = 0.7, n = 0$ (strong concentration of microelements) and $K = 0, 1, 2, 3$ when the flow is opposing

λ	$K = 0$		$K = 1$		$K = 2$		$K = 3$	
	$f''(0)$	$-\theta'(0)$	$f''(0)$	$-\theta'(0)$	$f''(0)$	$-\theta'(0)$	$f''(0)$	$-\theta'(0)$
1.0	0.691693	0.632369	0.511154	0.590372	0.416261	0.564685	0.359159	0.546612
1.1	0.631500	0.623645	0.475074	-0.254725	0.389801	0.588659	0.388030	0.541072
1.2	0.568678	-0.405912	0.438223	-0.289156	0.375358	0.581968	0.316543	0.535317
1.3	0.505996	-0.453656	0.400515	-0.319671	0.567279	-0.254227	0.294668	0.529326
1.4	0.440161	-0.494103	0.361850	-0.346585	0.558749	0.538043	0.272370	-0.232634
1.5	0.371788	-0.527666	0.322102	-0.370143	0.549700	-0.274886	0.249606	0.523074
1.6	0.300353	-0.554436	0.281115	-0.390435	0.540047	0.529357	0.249606	-0.247928
1.7	0.225110	-0.574153	0.238688	-0.407498	0.529678	-0.278511	0.226328	0.516531
1.8	0.144926	-0.586077	0.194558	-0.421255	0.518444	0.522638	0.202475	-0.261684
1.9	0.057921	-0.588648	0.148361	-0.431500	0.506137	0.514240	0.177974	0.509661
2.0	-0.038513	-0.578523	0.098578	-0.437848	0.492455	-0.068064	0.152736	-0.273943
2.1	-0.156470	-0.546830	0.452868	-0.439610	0.476928	0.485183	0.126644	0.494755
2.2	-0.369090	-0.425388	0.376639	-0.435532	0.458743	0.473714	0.099548	0.477863
2.3			-0.073826	-0.430919	0.438271	0.469898	0.071246	0.468433
2.4			-0.152753	-0.394921	0.409032	0.463151	0.041449	0.458152
2.5					0.244012	0.456361	0.009728	0.446794
2.6						0.442968	-0.313977	0.434017
2.7					-0.085702	0.407892	0.024618	0.419257
2.8					-0.148538	0.377329	-0.062885	0.401451
						0.318408	-0.287154	0.378072
							-0.173784	0.337624

Figures 12-14 show the dual solutions for the velocity, microrotation and temperature profiles when the flow is opposing with the mixed convection parameter $\lambda = 2$, $Pr = 0.7$ and $K = 0$ (Newtonian fluid), 1 and 3. It can be seen that the thickness of the dual hydrodynamic, microrotation and thermal boundary layers increase with the increase of K . It is worth mentioning that such dual solutions for the two-dimensional stagnation point flow of a micropolar fluid have not been reported before in the literature. As was pointed out by Afzal and Hussain (1984) for a Newtonian fluid ($K = 0$), and Nazar *et al.* (2003) for a micropolar fluid, it is plausible that the solution which occurs physically may depend on the manner in which the temperature field is imposed. However, in such problems where dual solutions occur then the upper solution curves (first dual solutions) are usually stable whilst the lower curves (the second dual solutions) are unstable.

Material parameter K	$f''(0) = 0$	λ	$-\theta'(0) = 0$
0	1.9608		1.5111
1	2.1837		1.7081
2	2.3194		1.8274
3	2.4290		1.9206

Table III.
Values of λ for the case of opposing flow when $f''(0) = 0$ and $-\theta'(0) = 0$ for $n = 0$, $Pr = 0.7$ and some values of K

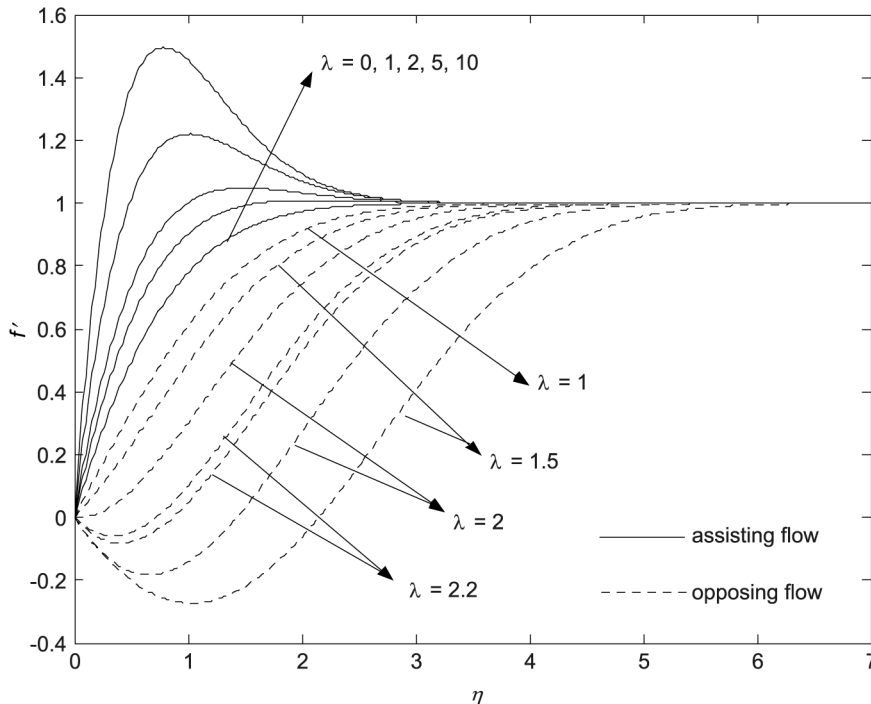


Figure 4.
Velocity profiles for $K = 0$ (Newtonian fluid), $Pr = 0.7$ and some values of λ

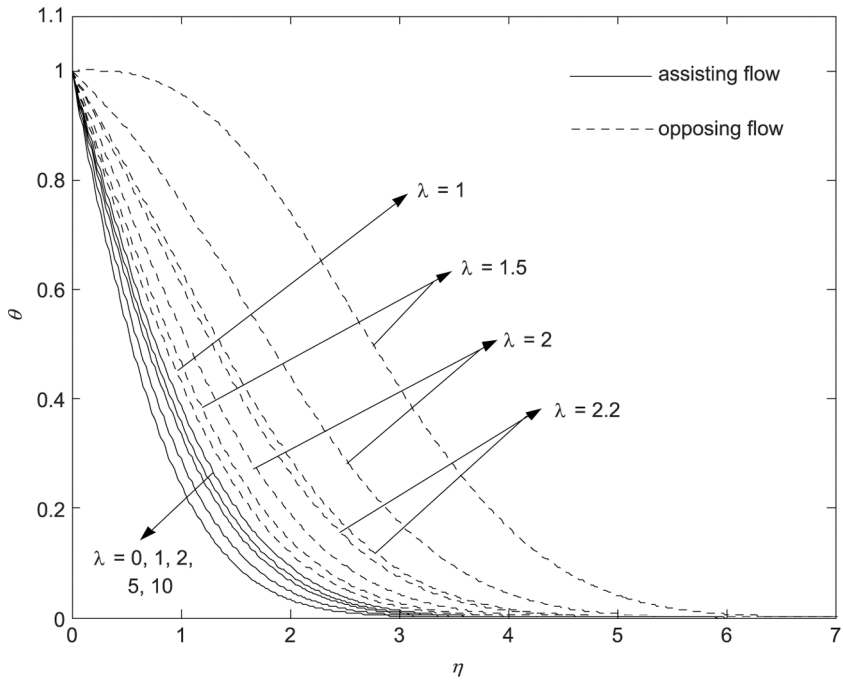


Figure 5.
Temperature profiles for
 $K = 0$ (Newtonian fluid),
 $Pr = 0.7$ and some
values of λ

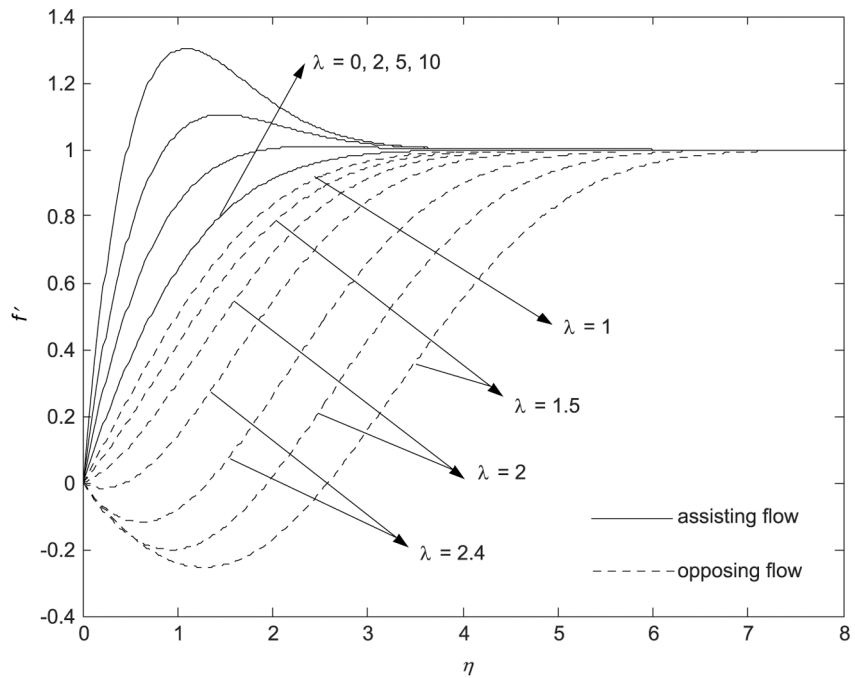


Figure 6.
Velocity profiles for
 $K = 1$, $Pr = 0.7$ and
some values of λ

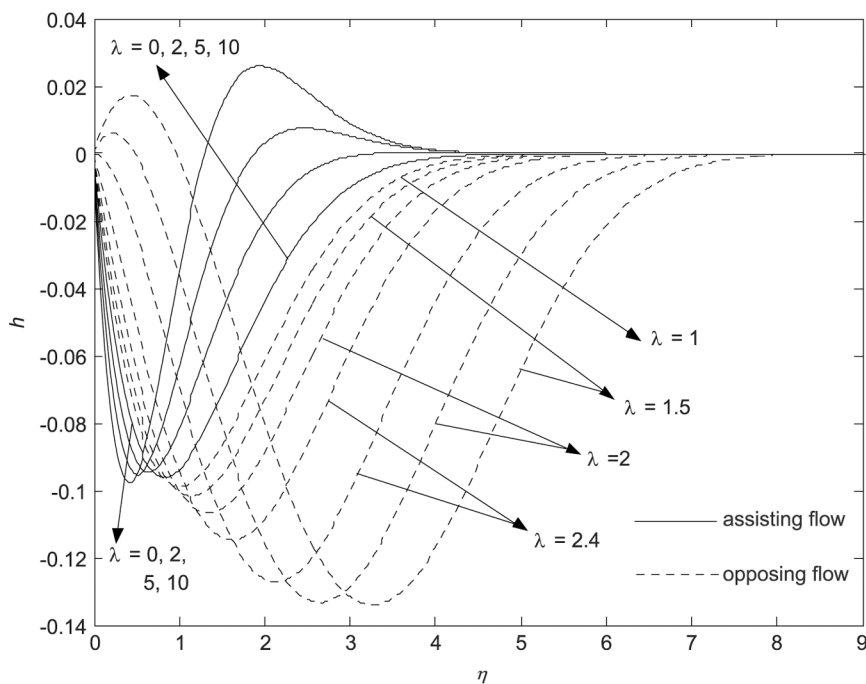


Figure 7. Microrotation profiles for $K = 1, Pr = 0.7$ and some values of λ

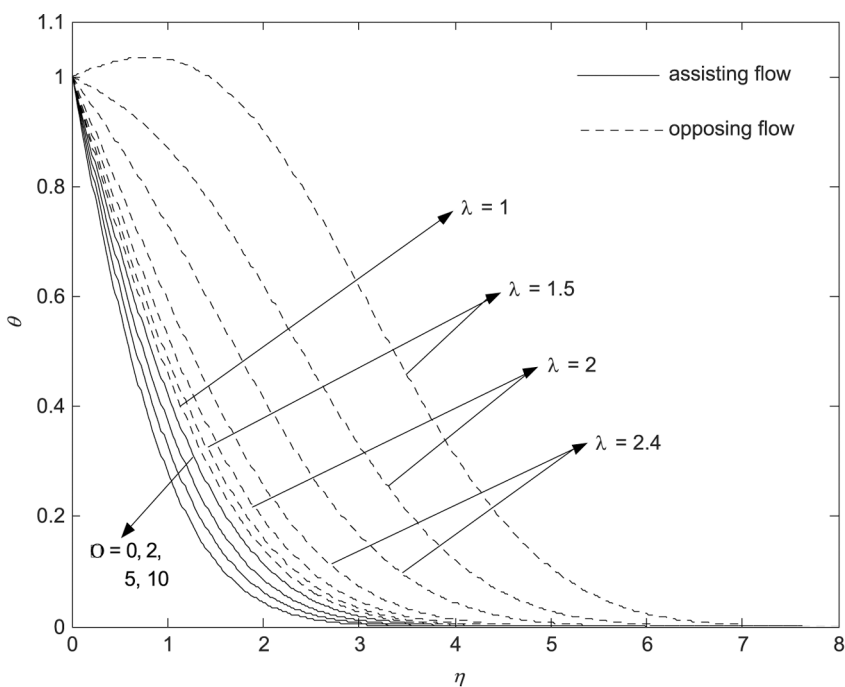


Figure 8. Temperature profiles for $K = 1, Pr = 0.7$ and some values of λ

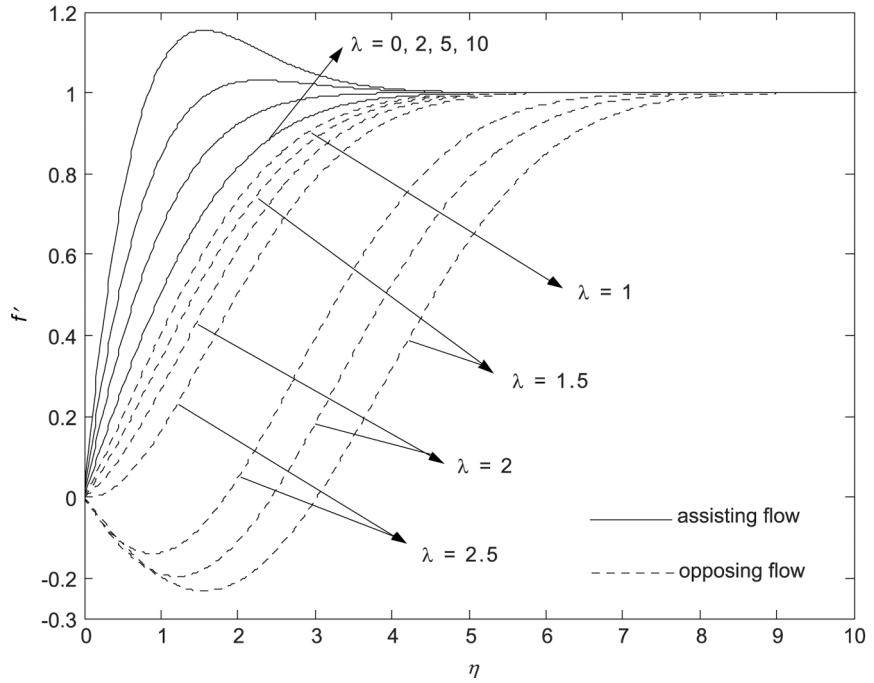


Figure 9.
Velocity profiles for
 $K = 3$, $Pr = 0.7$ and
some values of λ

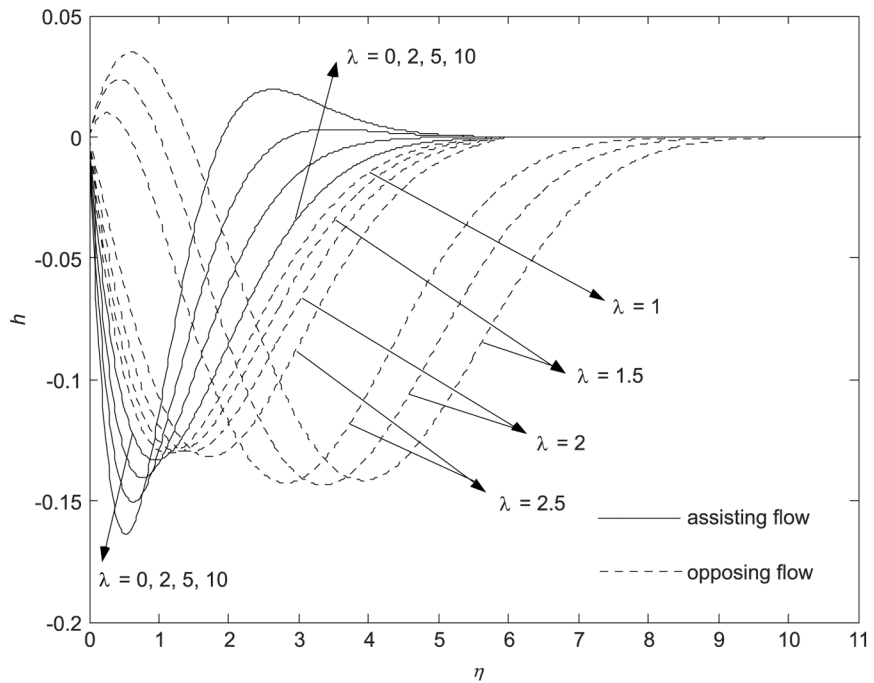


Figure 10.
Microrotation profiles for
 $K = 3$, $Pr = 0.7$ and
some values of λ

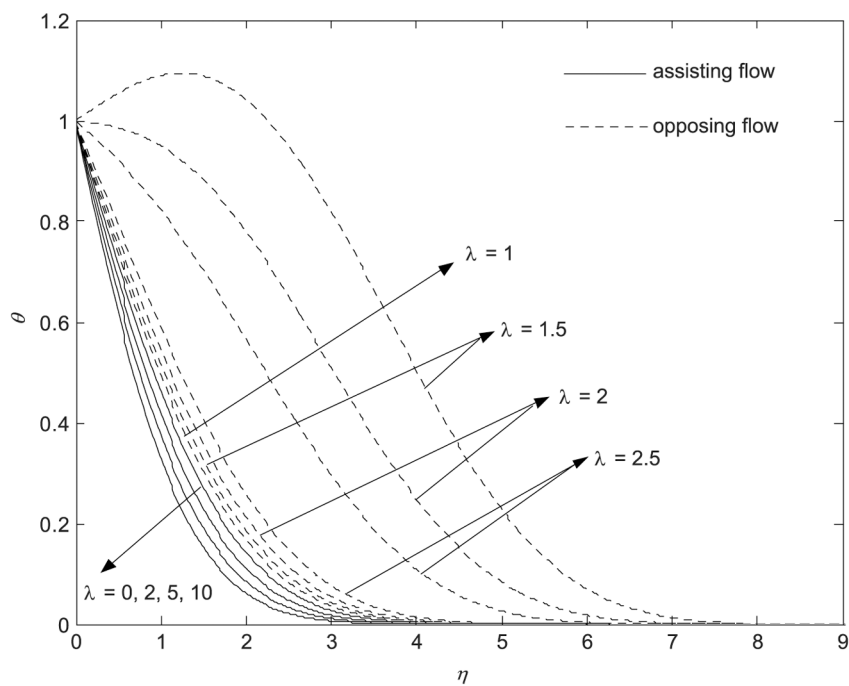


Figure 11.
Temperature profiles for
 $K = 3$, $Pr = 0.7$ and some
values of λ

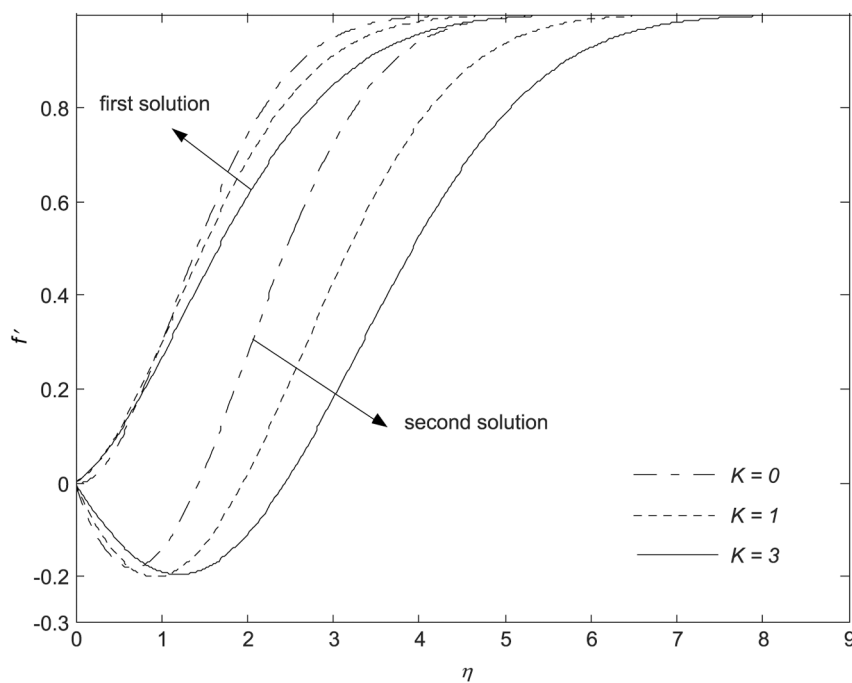


Figure 12.
Velocity profiles for $\lambda = 2$,
 $Pr = 0.7$ and some values
of K when the flow is
opposing

Figure 13.
Microrotation profiles for $\lambda = 2$, $Pr = 0.7$ and some values of K when the flow is opposing

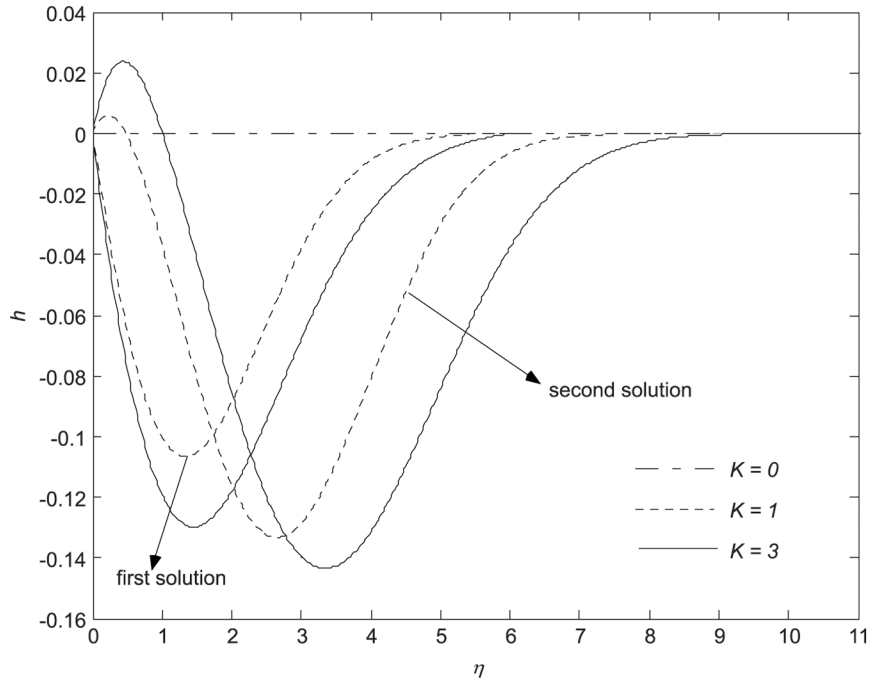
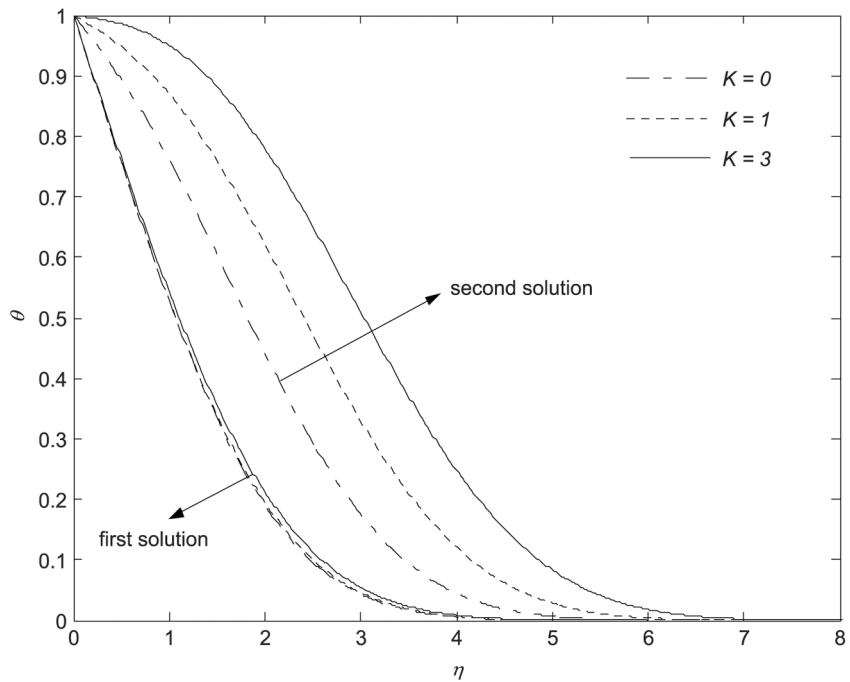


Figure 14.
Temperature profiles for $\lambda = 2$, $Pr = 0.7$ and some values of K when the flow is opposing



Conclusions

In this paper we have studied the problem of steady mixed convection boundary-layer flow of a micropolar fluid near the region of a stagnation point on a heated or cooled vertical surface. It is found that the governing partial differential equations become similar, i.e. reduce to ordinary differential equations, when the surface temperature of the plate varies linearly with the distance x along the plate. Numerical solutions of these ordinary differential equations have been presented for a the parameter $n = 0$ (strong concentration), some values of the Prandtl number Pr and over a range values of the material parameter K and the physically relevant mixed convection parameter values, $\lambda(\geq 0)$, which models the cases in which the buoyancy forces are both assisting and opposing the free stream. It is found for the opposing flow case that dual solutions exist and these solutions have been discussed in detail.

References

- Afzal, N. and Hussain, T. (1984), "Mixed convection over a horizontal plate", *ASME Journal of Heat Transfer*, Vol. 106, pp. 240-1.
- Ahmadi, G. (1976), "Self-similar solution of incompressible micropolar boundary layer flow over a semi-infinite plate", *International Journal of Engineering Science*, Vol. 14, pp. 639-46.
- Bergholz, R.F. (1980), "Natural convection of a heat generating fluid in a closed cavity", *ASME Journal of Heat Transfer*, Vol. 102, pp. 242-7.
- Cebeci, T. and Bradshaw, P. (1984), *Physical and Computational Aspect of Convective Heat Transfer*, Springer, New York, NY.
- Chandra Shekar, B., Vasseur, P., Robillard, L. and Nguyen, T.H. (1984), "Natural convection in a heat generating fluid bounded by two horizontal concentric cylinders", *Canadian Journal of Chemical Engineering*, Vol. 62, pp. 482-9.
- Cheng, C-Y. and Wang, C-C. (2000), "Forced convection in micropolar fluid flow over a wavy surface", *Numerical Heat Transfer, Part A*, Vol. 37, pp. 271-87.
- Eringen, A.C. (1966), "Theory of micropolar fluids", *Journal of Mathematics and Mechanics*, Vol. 16, pp. 1-18.
- Eringen, A.C. (1972), "Theory of thermomicropolar fluids", *Journal of Mathematical Analysis and Applications*, Vol. 38, pp. 480-96.
- Eringen, A.C. (2001), *Microcontinuum Field Theories. II. Fluent Media*, Springer, New York, NY.
- Gorla, R.S.R. (1983), "Micropolar boundary layer at a stagnation point", *International Journal of Engineering Science*, Vol. 21, pp. 25-34.
- Guram, G.S. and Smith, C. (1980), "Stagnation flows of micropolar fluids with strong and weak interactions", *Computers and Mathematics with Applications*, Vol. 6, pp. 213-33.
- Jena, S.K. and Mathur, M.N. (1981), "Similarity solutions for laminar free convection flow of a thermomicropolar fluid past a nonisothermal flat plate", *International Journal of Engineering Science*, Vol. 19, pp. 1431-9.
- Kumari, M. and Nath, N. (1984), "Unsteady incompressible boundary layer flow of a micropolar fluid at a stagnation point", *International Journal of Engineering Science*, Vol. 22, pp. 755-68.
- Łukaszewicz, G. (1999), *Micropolar Fluids: Theory and Application*, Birkhäuser, Basel.
- Nazar, R., Amin, N. and Pop, I. (2003), "Mixed convection boundary-layer flow from a horizontal circular cylinder in micropolar fluids: case of constant wall temperature", *International Journal of Numerical Methods for Heat and Fluid Flow*, Vol. 13, pp. 86-109.

HF
15,7

Peddieson, J. (1972), "An application of the micropolar fluid model to the calculation of turbulent shear flow", *International Journal of Engineering Science*, Vol. 10, pp. 23-32.

Peddieson, J. and McNitt, R.P. (1970), "Boundary layer theory for a micropolar fluid", *Recent Advances in Engineering Science*, Vol. 5, pp. 405-76.

Ramachandran, N., Chen, T.S. and Armaly, B.F. (1988), "Mixed convection in stagnation flows adjacent to vertical surfaces", *ASME Journal of Heat Transfer*, Vol. 110, pp. 373-7.

670

Rees, D.A.S. and Bassom, A.P. (1996), "The blasius boundary-layer flow of a micropolar fluid", *International Journal of Engineering Science*, Vol. 34, pp. 113-24.

Rees, D.A.S. and Pop, I. (1998), "Free convection boundary-layer flow of a micropolar fluid from a vertical flat plate", *IMA Journal of Applied Mathematics*, Vol. 61, pp. 179-97.

Willson, A.J. (1970), "Boundary-layer in micropolar liquids", *Proceedings of the Cambridge Philosophical Society*, Vol. 67, pp. 469-76.